Cancer-Associated Glycoforms of Gelatinase B Exhibit a Decreased Level of Binding to Galectin-3[†]

Simon A. Fry,[‡] Philippe E. Van den Steen,[§] Louise Royle,[‡,⊗] Mark R. Wormald,[‡] Anthony J. Leathem,[∥] Ghislain Opdenakker,[§] James M. McDonnell,[⊥] Raymond A. Dwek,[‡] and Pauline M. Rudd*[,‡,⊗]

Glycobiology Institute, Department of Biochemistry, University of Oxford, South Parks Road, Oxford OX1 3QU, U.K., Rega Institute for Medical Research, Laboratory of Immunobiology, University of Leuven, Minderbroedersstraat 10, B-3000 Leuven, Belgium, Department of Surgery, Royal Free and University College London Medical School, 67-73 Riding House Street, London W1W 1EJ, U.K., and Laboratory of Molecular Biophysics, Department of Biochemistry, University of Oxford, Oxford OX1 3QU, U.K.

Received June 23, 2006; Revised Manuscript Received September 4, 2006

ABSTRACT: Gelatinase B (MMP-9) and galectin-3 are widely known to participate in tumor cell invasion and metastasis. Glycans derived from MMP-9 expressed in MCF-7 breast cancer and THP-1 myeloid leukemia cells were compared with those from MMP-9 expressed in natural neutrophils. The many O-linked glycans of neutrophil gelatinase B presented a cluster of mainly galactosylated core II structures, 46% of which were ligands for galectin-3; 11% contained two to three *N*-acetyllactosamine repeating units that are high-affinity ligands for the lectin. The glycan epitopes thus provide MMP-9 with both high-affinity and (presumably) high-avidity interactions with galectin-3. In contrast, the *O*-glycans released from MMP-9 expressed in MCF-7 and THP-1 cells were predominantly sialylated core I structures. Only 10% of MCF-7 and THP-1 gelatinase B *O*-glycans were ligands for galectin-3 and contained only a maximum single *N*-acetyllactosamine repeat. Consistent with the glycan analysis, surface plasmon resonance binding assays indicated that the cancer-associated glycoforms of MMP-9 bound galectin-3 with an affinity and avidity significantly reduced compared with those of the natural neutrophil MMP-9. Galectin-3 exists as a multimer that also binds laminin, providing a means of localizing neutrophil MMP-9 in the extracellular matrix (ECM). The analytical data presented here suggest that MMP-9 glycoforms secreted by tumor cells are unlikely to be tethered at the site of secretion, thus promoting more extensive cleavage of the ECM and providing a rationale for the contribution that gelatinase B makes to cancer cell metastasis.

The matrix metalloproteases (MMPs)[1] are a family of Zn^{2+}-dependent endopeptidases (*1*) that are involved in extracellular matrix (ECM) remodeling in a variety of physiological and pathological processes. MMP degradation of ECM proteins is associated with many aspects of cancer progression, including cancer cell growth, differentiation, apoptosis, migration, and invasion, as well as regulation of angiogenesis and immune surveillance (*2*).

Gelatinase B (MMP-9) is a key regulator and effector of immunity (*3*, *4*). Like other MMPs, MMP-9 contains a prodomain (proteolytically removed to yield active enzyme), an active domain, and a zinc-binding domain. In addition, gelatinase B also contains a gelatin-binding fibronectin domain, an O-glycosylated domain, and a carboxy-terminal hemopexin domain. No complete crystal structure of gelatinase B exists; however, gelatinase B shares considerable sequence homology with gelatinase A. A model of gelatinase B (Figure 1) has been generated by inserting the Ser, Thr, and Pro rich collagen-type V-like domain into the crystallographic data of gelatinase A (*5*). Recent ultracentrifugation data (*6*) exclude the possibility that the O-glycosylated domain adopts an extended conformation. Natural gelatinase B from human neutrophils is heavily glycosylated (*7*, *8*). MMP-9 contains three consensus sequences for the attachment of N-linked glycans, only two of which are occupied (*9*, *10*), one in the prodomain (Asn_{38}-Leu-Thr) and one in the active domain (Asn_{120}-Ile-Thr or Asn_{127}-Tyr-Ser, SWIS-

[†] S.A.F. was supported by a D. Phil Studentship from Against Breast Cancer (1020967). This study was supported by the Glycobiology Institute Endowment, the Cancer Research Foundation of Fortis AB Insurances, The Belgian Federation against Cancer, the FWO-Vlaanderen, and the Concerted Research Actions (GOA 2002-2006 and 2006-2010). P.E.V.d.S. is a postdoctoral fellow of the FWO-Vlaanderen.

* To whom correspondence should be addressed. E-mail: Pauline.rudd@nibrt.ie. Telephone: +353 1 716 6728.

[‡] Glycobiology Institute, Department of Biochemistry, University of Oxford.

[§] University of Leuven.

[∥] Royal Free and University College London Medical School.

[⊥] Laboratory of Molecular Biophysics, Department of Biochemistry, University of Oxford.

[⊗] Present address: Dublin-Oxford Glycobiology Lab, NIBRT, Conway Institute, University College Dublin, Dublin, Ireland.

[1] Abbreviations: 2-AB, 2-aminobenzamide; ABS, *Arthrobacter ureafaciens* sialidase; AMF, almond meal fucosidase; BKF, bovine kidney α-fucosidase; BTG, bovine testes *β*-galactosidase; CRD, carbohydrate recognition domain; ECM, extracellular matrix; IL-8, interleukin-8; LN, *N*-acetyllactosamine; LPS, lipopolysaccharide; MMP, matrix metalloproteinase; NP-HPLC, normal phase high-performance liquid chromatography; PMA, phorbol myristate acetate; PNGase F, peptide *N*-glycosidase F; SPR, surface plasmon resonance; TIMP-1, tissue inhibitor of metalloproteinase-1.

10.1021/bi061254l CCC: $33.50
Published on Web 12/06/2006

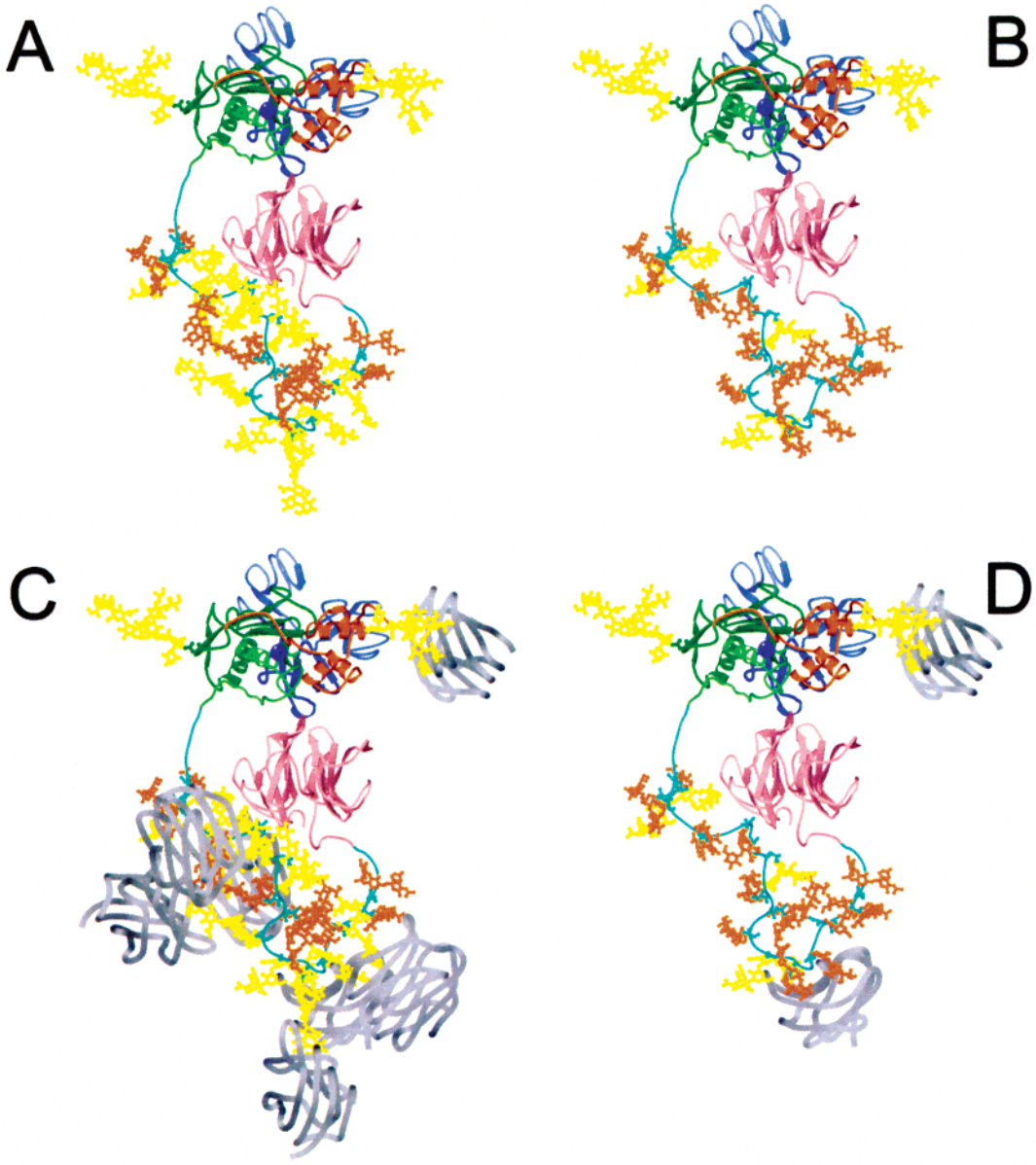

FIGURE 1: Molecular models of gelatinase B. Molecular models of gelatinase B from neutrophils and MCF-7 cells, based on the crystallographic studies, ultracentrifugation data, and glycan sequencing: orange for the propeptide domain, green for the zinc-binding and active site domains, dark blue for the fibronectin domains, light blue for the OG domain, pink for the hemopexin domain, purple for the zinc ion in the active site, yellow for N-linked and O-linked glycans containing galectin binding epitopes, and orange for O-linked glycans without galectin binding epitopes. (A) Neutrophil gelatinase B. (B) MCF-7 gelatinase B. (C) Complex of neutrophil gelatinase B with six galectin-3 CRDs. (D) Complex of MCF-7 gelatinase B with two galectin-3 CRDs.

SPROT numbering scheme).

Gelatinase B is typically stored in large amounts in neutrophil granules to allow rapid release in the innate immune responses (*11*). Expression levels are increased in many cancer cell types, including breast carcinomas (*12*). Gelatinase B is a member of the protease cascade that cleaves ECM proteins, and it is required for effective cell invasion and metastasis (*13*, *14*).

Galectin-3 is connected to the biology of MMPs in several ways under normal and pathological conditions, e.g., downstream regulation of MMP-9 during bone formation (*15*). In addition, galectin-3 has been shown to play various roles in cancer metastasis (*16*), e.g., by interacting with sugars in the fibronectin protein (*17*). Galectin-3 is localized on various cell surfaces, presumably by interacting with cell-surface glycoproteins displaying sugars with terminal galactose residues (*18*). The suggestion is that galectin-3 would tether MMP-9 to the cell surface under normal conditions. In the tumor situation, the aberrant glycosylation makes this less likely and consistent with the proposal that the altered glycans allow cells to detach from the ECM.

Galectin-3 is a 30 kDa β-galactose binding lectin that has a carboxy-terminal carbohydrate recognition domain (CRD) (*19*) and a flexible Pro, Tyr, and Gly rich amino-terminal domain that contains the gelatinase B cleavage site. This amino-terminal collagen-like domain is required for the noncovalent self-association of two to five galectin-3 molecules (*20*−*22*). Multimeric galectin-3 cross-links glycoproteins carrying glycans terminating in galactose, such as laminin and MMP-9. Cleavage of the Ala_{62}−Tyr_{63} bond of galectin-3 by gelatinase B reduces the level of self-association and thus abrogates processes dependent on this (*23*).

Aberrant glycosylation is a common feature of cancer that can significantly modulate the functions of the proteins to which they are attached (*24*−*28*). Here, the glycosylation of natural neutrophil gelatinase B has been compared with that of gelatinase B secreted from MCF-7 breast cancer cells and THP-1 myeloid leukemia cells. As a result, fewer core 2 O-linked glycans were found on the MCF-7 and THP-1 gelatinase B. The decrease in the level of binding of galectin-3 to MMP-9 glycoforms secreted by tumor cells, determined by surface plasmon resonance, may provide a rationale for the contribution that gelatinase B makes to the cancer-associated processes of invasion and metastasis.

RESULTS

Production of Cancer-Associated Glycoforms of Gelatinase B. Phorbol myristate acetate (PMA) upregulates expression levels of gelatinase B in many cell types by directly activating protein kinase C (PKC) (*11*, *29*, *30*). Activated PKC influences signal transduction, leading to enhanced transcription of the gelatinase B gene (*29*). Lipopolysaccharide, a bacterial cell wall component with a major immunostimulatory role in Gram-negative infections, is another inducer of gelatinase B (*31*), which acts mainly on leukocytes through the action of the LPS receptors CD14 and/or Toll-like receptor-4.

MCF-7 breast cancer cells were therefore incubated in serum free medium in the presence of a range of LPS and PMA concentrations. For each condition, 10 μL of medium was tested for gelatinase levels by gelatin zymography (Figure 2). Treatment with LPS did not result in any induction of gelatinase B (92 kDa) expression after 48 h (Figure 2A), while gelatinase A (70 kDa) was constitutively present. Considerable gelatinase B expression levels were achieved by incubating MCF-7 cells in the presence of PMA after 24, 48, or 72 h, and the highest levels were obtained with 10−100 ng/mL PMA after 48 h (Figure 2B). Comparisons of dilutions of the culture fluids of induced MCF-7 cells with undiluted MCF-7 supernatants indicate that the expression of gelatinase B is approximately 500-fold enhanced by PMA, compared to the low but detectable basal expression level (Figure 2C), as measured by zymography. Furthermore, this analysis allowed for a careful comparison of the relative molecular mass of gelatinase B and showed that the MW of the MCF-7 gelatinase B was slightly lower than that of gelatinase B from neutrophils and higher than that of recombinant gelatinase B produced in Sf9 insect cells (*6*). Furthermore, it is clear that the MW did not change upon induction with PMA. These data provide a first indication that the size of the N- and O-linked glycans of MCF-7 gelatinase B is intermediate between the relatively large sugars of neutrophil gelatinase B (*8*) and the small sugars found on recombinant gelatinase B from insect cells (*6*). The data also suggest that no major changes in the number and size of glycans per molecule of gelatinase B occur upon induction with PMA.

In the leukemic THP-1 cell line, considerable induction of gelatinase B was obtained with both PMA and LPS, as expected (*31*). The induction of THP-1 cells with different concentrations of LPS after 48 h is shown in Figure 2D and indicates that (1) the MW of THP-1 gelatinase B is also intermediate between that of neutrophil and recombinant Sf9 gelatinase B and (2) without inducer, no gelatinase B was detected.

Large-scale production of MCF-7 gelatinase B was obtained by stimulating liters of MCF-7 cell culture with PMA, and the resulting supernatant was purified by gelatin affinity chromatography. For the production of THP-1 gelatinase B, LPS was chosen as a physiological inducer. Panel E in Figure 2 shows protein staining with Coomassie Blue of the purified preparations from MCF-7 and THP-1 tumor cells. In both cases, the purified material contained tissue inhibitor of metalloproteinase-1 (TIMP-1) (Figure 2E), as did the THP-1 gelatinase B (*31*). TIMP-1 contains two N-linked glycosylation sites but no reported *O*-glycans.

Analysis of the N-Linked Glycans of Gelatinase B. A final purification step to separate TIMP-1 from gelatinase B was carried out via reducing SDS−PAGE (Figure 2E). *N*-Glycans were released directly from gel bands containing gelatinase B by incubation with PNGaseF. Each glycan pool was subsequently labeled with 2-aminobenzamide (2-AB) and resolved by normal phase high-performance liquid chromatography (NP-HPLC). By comparison with a standard dextran hydrolysate ladder, oligosaccharide elution positions could be expressed as glucose units (GU). Preliminary structures of oligosaccharides were assigned by reference to the GU values of a database of standard sugars (*32*) and confirmed by using a series of parallel exoglycosidase array digestions (Figure 3A,B).

Core fucosylated complex-type biantennary *N*-glycans were detected on both THP-1 and MCF-7 gelatinase B. The nonreducing termini of THP-1 gelatinase B *N*-glycans were more heavily sialylated (α2−3- and α2−6-linked) than those of MCF-7 gelatinase B but carried less outer arm fucose (α1−3GlcNAc). Triantennary and bisected triantennary *N*-glycans were detected following sialidase (ABS) treatment (Figure 3B and Table 2). The MCF-7 gelatinase B *N*-glycan sialic acids were all α2−3-linked, and outer arm fucose was present in α1−2Gal and α1−3GlcNAc linkages (Figure 3A and Table 1). *N*-Glycan analysis of neutrophil gelatinase B was carried out previously by Rudd et al. (*8*). More than 95% were partially sialylated, core fucosylated biantennary structures with and without outer arm α1−3-linked fucose. No *N*-acetyllactosamine structures were identified.

Analysis of the O-Linked Glycans of Gelatinase B. O-Linked glycans were released from gelatinase B by optimized hydrazinolysis at 60 °C for 6 h. Structures of the 2-AB-labeled *O*-glycans were assigned from their GU values and the result of exoglycosidase digestions. Figure 4 demonstrates that there is little variation in O-glycosylation between MCF-7 and THP-1 gelatinase B. All of these relatively small *O*-glycans are heavily sialylated, and no fucosylation was detected. Sialylated core I *O*-glycans (Galβ1−3GalNAc) were the most abundant, and monosialylated and disialylated core I was present in both cases. The remaining *O*-glycans were all of the galactosylated core II-type (Galβ1−4GlcNAcβ1−6[Galβ1−3]GalNAc) further modified by one or two sialic acids. The *O*-glycans of neutrophil gelatinase B were analyzed by Mattu et al. (*7*) and mainly consisted of type II cores with lactosamine extensions, with or without sialic acid or outer arm fucose.

Lactosamine extensions on oligosaccharides are often important functional determinants and are, in particular, good ligands for galectin-3. Therefore, the relative percentages of

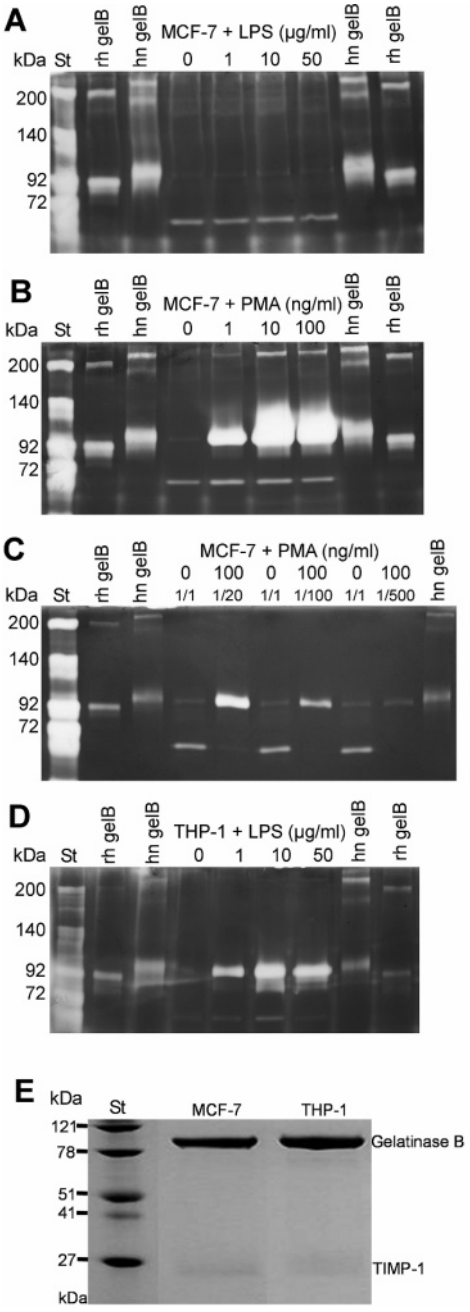

FIGURE 2: Production of cancer-associated glycoforms of gelatinase B. MCF-7 cells were grown to 80% confluence and then incubated in serum free medium for 48 h in the presence of different concentrations of LPS (A) or PMA (B); 10 μL of medium was tested by gelatin zymography and compared with gelatinase B from human neutrophils (hn gelB) and with recombinant human gelatinase B produced in Sf9 insect cells (rh gelB). White bands on the Coomassie blue-stained zymogram indicate the presence of gelatinase activity. Gelatinase B migrates at a relative molecular mass of ~90 kDa, whereas gelatinase A (approximately 72 kDa) is constitutively expressed. (C) Comparison of 1:20, 1:100, and 1:500 dilutions of MCF-7 cell supernatans induced with 100 ng/mL PMA with gelatinase B and gelatinase A in the undiluted supernatants of uninduced MCF-7 cells and with gelatinase B from human neutrophils or recombinant Sf9 gelatinase B. (D) THP-1 cells were induced with different concentrations of LPS, and the gelatinases in the supernatants were analyzed with gelatin zymography and compared with natural neutrophil and recombinant Sf9 gelatinase B. (E) Reducing SDS−PAGE of 5 μg of material purified from MCF-7 and THP-1 cells by gelatin−Sepharose affinity chromatography shows the presence of purified gelatinase B and TIMP-1.

glycans containing one, two, or three lactosamine units (repeats) were calculated for the glycoforms of neutrophil gelatinase B (*7*) and for the glycoforms of THP-1 and MCF-7 gelatinase B (Figure 5).

Lactose Inhibits Binding of Galectin-3 to Gelatinase B. This interaction of gelatinase B with galectin-3 was shown to be mediated by the sugars in inhibition assays using lactose (a galectin-3 ligand); 96-well plates were coated with human recombinant galectin-3 before addition of 100 ng of gelatinase B and increasing concentrations of lactose. Bound gelatinase B was eluted and detected by zymography (Figure 6). The data indicate that gelatinase B is a ligand for galectin-3 and that lactose inhibits binding of galectin-3 to neutrophil, THP-1, and MCF-7 gelatinase B, consistent with galectin-3 binding to gelatinase B glycans.

MMP-9 Binds the CRD of Galectin-3. The extended non-CRD N-terminal domain of galectin-3 has a collagen-like structure and contains a gelatinase B cleavage site; therefore, both protein−protein and protein−carbohydrate interactions with galectin-3 may be involved in the binding to gelatinase B. Galectin-3 was therefore digested with *Clostridium histolyticum* collagenase type II to yield an NH_2-terminally truncated form of galectin-3 (galectin-3C) which contains an intact CRD but lacks the gelatinase B cleavage site; 96-well plates were coated with either human recombinant galectin-3 or galectin-3C before addition of 100 ng of gelatinase B and 40 mM lactose or sucrose. Bound gelatinase B was eluted and detected by zymography (Figure 7). Data in Figure 7 show that lactose but not sucrose inhibits the binding of neutrophil gelatinase B to galectin-3 (lanes 2 and 3) and also to galectin-3C (lanes 5 and 6). These data are consistent with a specific lectin−carbohydrate interaction between gelatinase B and the galectin-3 CRD.

Quantitative Analysis of Galectin-3 Binding to Gelatinase B. Surface plasmon resonance (SPR) was used to measure the affinities and stoichiometries of binding of galectin-3 to the different gelatinase B samples. Purified gelatinase B from THP-1, MCF-7, and neutrophils was immobilized on a sensor surface, thus normalizing the concentrations, and binding was analyzed over a range of galectin-3 concentrations. Binding affinities of galectin-3 for THP-1- and MCF-1-derived gelatinase B were similar (K_ds of 800 and 900 nM, respectively) with a modest increase in the B_{max} values for the MCF-7 material (440 vs 560 resonance units) (Figure 8A,B). The binding characteristics of galectin-3 for the neutrophil-derived gelatinase B were distinctly different (Figure 8C); it exhibited a markedly higher overall B_{max} (2100 RU) with a slightly weaker K_d (3 μM) and has a minor component of binding that has a significantly higher affinity (110 nM with a B_{max} of 170 RU).

DISCUSSION

Gelatinase B Glycosylation. The glycoforms of MCF-7 and THP-1 gelatinase B have shorter oligosaccharide chains than natural neutrophil gelatinase B. Such short glycan chains are a common feature of cancer cell proteins and give an indication that normal glycosylation pathways have often been disrupted in cancer cells. In breast cancer, for example, MUC1 *O*-glycans are core I rather than core II-type structures. This is the result of an increased level of expression of a sialyltransferase that competes with a core

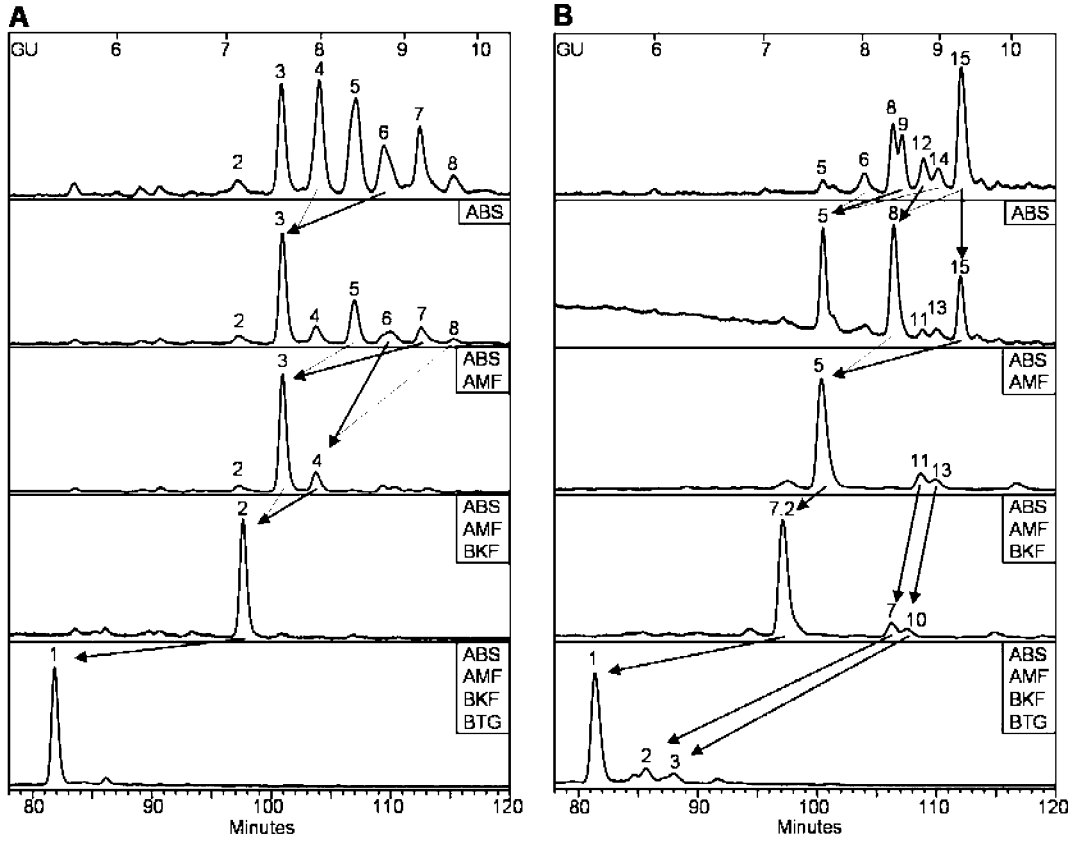

Peak No.	GU	Structure	% N-glycan pool: Undigested	ABS	ABS AMF	ABS AMF BKF	ABS AMF BKF BTG
1	5.5	A2	-	-	-	-	100.0
2	7.2	A2G2	-	-		100.0	-
3	7.6	FcA2G2	19.3	46.3	84.0	-	-
4	8.0	FcA2G2F(2)	23.6	9.8	16.0	-	-
		FcA2G2S(3)		-	-	-	-
5	8.4	FcA2G2F(3)	23.6	21.4	-	-	-
6	8.8	FcA2G2F2(2,3)	13.8	10.4	-	-	-
		FcA2G2S2(3,3)		-	-	-	-
7	9.2	FcA2G2F2(3,3)	15.2	9.3	-	-	-
8	9.7	FcA2G2F3(2,3,3)	4.5	2.8	-	-	-

Peak No.	GU	Structure	% N-glycan pool: Undigested	ABS	ABS AMF	ABS AMF BKF	ABS AMF BKF BTG
1	5.5	A2	-	-	-	-	77.1
2	5.9	A3	-	-			11.5
3	6.1	A3B	-	-	-	-	11.4
4	7.2	A2G2	-	-	-	86.1	-
5	7.6	FcA2G2	2.7	30.6	82.0	-	-
6	8.0	FcA2G2S(3)	6.3	-	-	-	-
7	8.3	A3G3	-	-	-	9.1	-
8	8.4	FcA2G2F(3)	16.9	42.5	-	-	-
9	8.5	FcA2G2S(6)	15.1	-	-	-	-
10	8.6	A3G3B	-	-	-	5.8	-
11	8.7	FcA3G3	-	2.4	10.5	-	-
12	8.8	FcA2G2F(3)S(3)	11.0	-	-	-	-
13	8.9	FcA3G3B	-	4.2	7.5	-	-
14	9.0	FcA2G2S2(3,6)	8.1	-	-	-	-
15	9.2	FcA2G2F(3)S(6)	39.9	-	-	-	-
		FcA2G2F2(3,3)		20.3	-	-	-

FIGURE 3: Structural analysis of (A) MCF-7 gelatinase B *N*-glycans and (B) THP-1 gelatinase B *N*-glycans. 2-AB-labeled oligosaccharides released from gelatinase B by PNGase F in gel digestion were resolved by NP-HPLC. Glycan structures were determined from their elution position (measured in GU) by comparison with GU values of a database of standard glycans. Assignments were confirmed using simultaneous exoglycosidase arrays of known specificity. Arrows indicate the shift of peaks following digestion with enzyme arrays. The major peaks (those with peak areas of >2%) have been annotated and assigned. ABS is *A. ureafaciens* sialidase (removes α2−3 or −6-linked sialic acid), AMF almond meal fucosidase (α1−3 or −4-linked Fuc), BKF bovine kidney fucosidase (α1−6 or −2-linked Fuc), and BTG bovine testes galactosidase (*β*1−3 or −4-linked Gal). Structural abbreviations are as follows. All *N*-glycans have two core GlcNAcs: Fc, Fucα1−6 linked to inner core GlcNAc; A*x*, number (*x*) of antennae (GlcNAc) on the trimannosyl core; B, bisecting GlcNAc (linked *β*1−4 to inner mannose); G*x*, number (*x*) of Gals on antennae; F*x*, number (*x*) of Fucs on antennae; S*x*, number (*x*) of sialic acids on antennae; linkage of outer arm Fuc (α1−2 or α1−3) and sialic acid (α2−3 or α2−6) shown in parentheses.

II GlcNAc transferase for their shared core I substrate (*33*). This decrease in core 2 structures, however, may not be generalized for all cancer cell types, as, e.g., in colonic carcinoma core II GlcNAc tranferase it was found to be increased (*34*). The altered glycosylation status of both secreted and cell-surface glycoproteins can endow the proteins with alternative properties that can aid tumor progression. For example, an increased degree of *β*1−6GlcNAc branching (mediated by UDP-GlcNAc α-mannose *β*1−6-*N*-acetylglucosaminyltransferase) leads to increased resistance of matriptase to degradation (*35*). This in turn enhances matrix metalloproteinase activation and metastasis (*36*, *37*).

Glycans of Gelatinase B Bound by Galectin-3. Gelatinase B contains two N-linked glycans and 18 potential O-glycosylation sites in the 56-residue O-glycosylated domain (as predicted by the NetOGlyc 3.1 server, www.cbs.dtu.dk/services/NetOGlyc/). Several factors implicate the O-linked glycans as the source of variations in the interaction between galectin-3 and gelatinase B of various origins. First, galec-

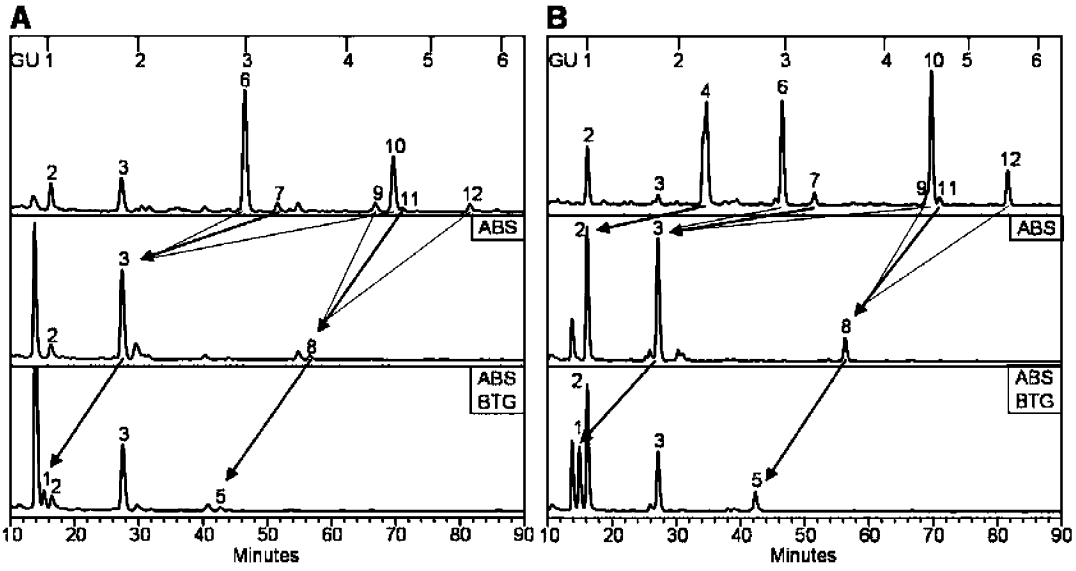

Peak	GU	Structure	% O-glycan pool		
			Undigested	ABS	ABS BTG
1	0.9		-	-	15.1
2	1.0		9.5	14.4	15.3
3	1.8		12.5	81.1	65.1
4	ND	ND	-	-	-
5	2.7		-	-	4.5
6	3.0		45.4	-	-
7	3.3		3.4	-	-
8	3.6		-	4.5	-
9	4.3		4.2	-	-
10	4.5		20.6	-	-
11	4.6		1.4	-	-
12	5.5		3.0	-	-

Peak	GU	Structure	% O-glycan pool		
			Undigested	ABS	ABS BTG
1	0.9		-	-	21.8
2	1.0		10.7	44.8	44.3
3	1.8		2.1	45.8	24.3
4	2.3		21.9	-	-
5	2.7		-	-	9.6
6	3.0		22.7	-	-
7	3.3		3.2	-	-
8	3.6		-	9.4	-
9	4.5		2.0	-	-
10	4.5		27.9	-	-
11	4.6		1.7	-	-
12	5.5		7.8	-	-

FIGURE 4: Analysis of (A) MCF-7 gelatinase B *O*-glycans and (B) THP-1 gelatinase B *O*-glycans. 2-AB-labeled oligosaccharides released from gelatinase B by manual hydrazinolysis were resolved by NP-HPLC. Glycan structures were determined from their elution position (measured in GU) by comparison with GU values of a database of standard glycans. Assignments were confirmed using simultaneous exoglycosidase arrays of known specificity. Arrows indicate the shift of peaks following digestion with enzyme arrays. The major peaks have been annotated and assigned. Peak 4 is the result of degradative peeling (*32*). ABS is *A. ureafaciens* sialidase (removes α2−3 or −6-linked sialic acid) and BTG bovine testes galactosidase (*β*1−3 or −4-linked Gal). Note that BTG removes only the Gal*β*1-3 from 2AB-labeled GalNAc of core 1 with very low efficiency due to the GalNAc being in the open-ring form (*32*). The scheme for glycan representation is as follows: (♦) *N*-acetylgalactosamine, (◊) galactosamine, (■) *N*-acetylglucosamine, (★) sialic acid, (dashed line) α-linkage, (solid line) *β*-linkage, (\) 1−6 linkage, (—) 1−4 linkage, (/) 1−2 linkage. ND means not detected.

tin-3 is more likely to encounter an *O*-glycan since these are more abundant than the two *N*-glycans. The 18 potential O-glycosylation sites, most of which are predicted to be occupied (*8*), present multiple ligands for galectin-3 in a binding domain. Galectin-3 has affinity for lactosamine disaccharides (Gal*β*1−4GlcNAc); it recognizes the 4- and 6-OH groups of Gal and the 3-OH group of GlcNAc. This affinity dramatically increases in response to increases in the number of repeating *N*-acetyllactosamine (LN) units in the substrate, i.e., LN (K_d = 26 μM), LN2 (K_d = 1.3 μM), and LN3 (K_d = 0.35 μM) (*38*). Neutrophil gelatinase B *O*-glycans (ranging from 2 to 10 monosaccharides) consist of the following: 35% of the structures with one *N*-acetyllactosamine unit, 8% with two *N*-acetyllactosamine units, and 3% with three *N*-acetyllactosamine repeats. MCF-7 and THP-1 have less than 10% of their glycans with one *N*-acetyllactosamine and none with more (Figure 5). Therefore, compared with gelatinase B from the cancer cell lines, neutrophil gelatinase B has nearly 10 times as many multiply presented ligands for galectin-3. This may be assumed to increase the avidity of the interaction between neutrophil gelatinase B and galectin-3 (although the avidity was not measured in this study). In addition, many of these ligands have a higher affinity for the lectin, as they contain more *N*-acetyllactosamine units.

Interaction between Galectin-3 and Gelatinase B. The glycan analysis, SPR data, and zymography assays were all consistent with binding of the galectin-3 CRD to the

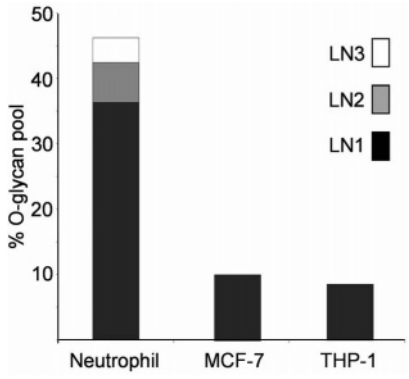

FIGURE 5: Relative proportions of gelatinase B *O*-glycans containing lactosamine. Gelatinase B *O*-glycans that contain lactosamine are shown as a percentage of the entire *O*-glycan pool: LN1, *O*-glycans containing one *N*-acetyllactosamine repeat; LN2, *O*-glycans containing two *N*-acetyllactosamine repeats; and LN3, *O*-glycans containing three *N*-acetyllactosamine repeats.

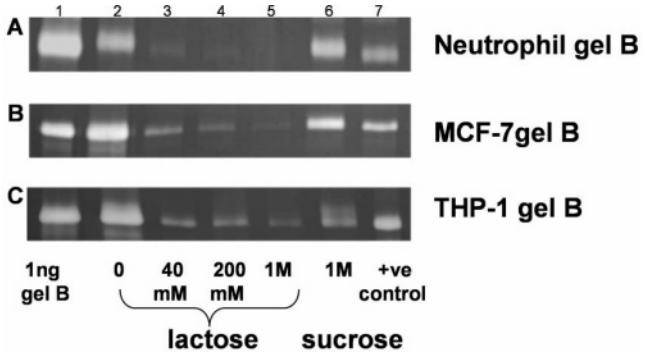

FIGURE 6: Lactose inhibits binding of galectin-3 to gelatinase B: (A) neutrophil gelatinase B, (B) MCF-7 gelatinase B, and (C) THP-1 gelatinase B. ELISA plates (96 wells) were coated with 2.5 μg of galectin-3 (or gelatin as a control); 100 ng of gelatinase B was added in the presence of lactose or sucrose (negative control). Bound gelatinase B was eluted with loading buffer and visualized by gelatin zymography. White bands on the Coomassie blue-stained zymogram indicate gelatinolytic activity: lane 1, 1 ng of gelatinase B; lane 2, gelatinase B bound by galectin-3 in the presence of 0 mM lactose; lane 3, gelatinase B bound by galectin-3 in the presence of 40 mM lactose; lane 4, gelatinase B bound by galectin-3 in the presence of 200 mM lactose; lane 5, gelatinase B bound by galectin-3 in the presence of 1 M lactose; lane 6, gelatinase B bound by galectin-3 in the presence of 1 M sucrose; and lane 7, positive control (well coated with gelatin).

O-glycans of gelatinase B. The number of saturatable binding sites determined by SPR was also consistent with the comparative glycan analyses of gelatinase B derived from THP-1 cells, MCF-7 cells, and neutrophils (Figure 5). The high-affinity site observed for binding of galectin-3 to neutrophil-derived gelatinase B can be ascribed to the presence of tetra- and hexasaccharide moieties in this sample. The zymography assays, although not quantitative, indicated that the binding of gelatinase B to galectin-3 can be inhibited by lactose [*O*-β-D-galactopyranosyl-(1−4)-β-D-glucopyranose], an established ligand for galectin-3. In contrast, sucrose, which is a disaccharide consisting of glucose and fructose, did not inhibit the binding.

Altered Gelatinase B Glycosylation and Reduction of the Level of Galectin-3 Binding in Cancer May Engage in Widespread Degradation of the ECM. An important aspect of tumorigenesis is basement membrane and extracellular matrix degradation. Gelatinase B is implicated in this process

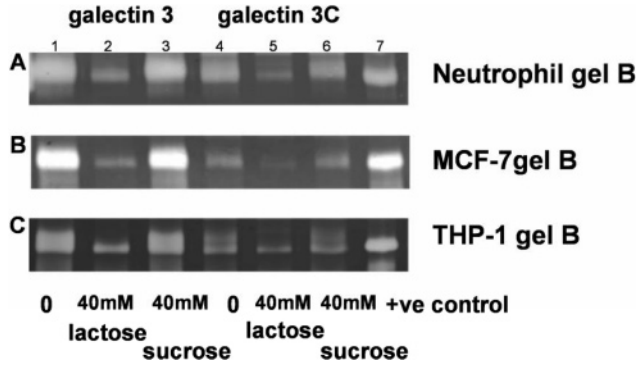

FIGURE 7: Gelatinase B binds collagenase-treated galectin-3: (A) neutrophil gelatinase B, (B) MCF-7 gelatinase B, and (C) THP-1 gelatinase B. Lanes 1−3 show wells coated with 2.5 μg of galectin-3 and lanes 4−6 wells coated with 2.5 μg of galectin-3C, and lane 7 shows a positive control (well coated with gelatin); 100 ng of gelatinase B was added in the presence of 40 mM lactose (lanes 2 and 5) or sucrose (lanes 3 and 6). Bound gelatinase B was eluted with loading buffer and visualized by gelatin zymography. White bands on the Coomassie blue-stained zymogram indicate gelatinolytic activity.

in experimental metastasis assays demonstrating that fewer colonies are formed in the lungs of mice when gelatinase B is downregulated in cancer cells (*13*) and when MMP-9-null mice are compared to wild-type mice (*14*). The role of gelatinase B glycosylation on in vivo metastasis of either MCF-7 and THP-1 cells remains unknown because in vitro, MCF-7 cells express only small amounts of gelatinase B and THP-1 cells fail to express gelatinase B spontaneously. Further studies are required to determine whether and by which agonists gelatinase B expression is induced in these forms of cancer in vivo. During inflammation, interleukin-8 (IL-8) is produced by various cell types and acts as both a neutrophil chemoattractant and an inducer of degranulation of gelatinase B. Neutrophil gelatinase B potentiates IL-8 by amino-terminal clipping, thus providing a positive feedback loop (*39*). Galectin-3-mediated sequestration of neutrophil gelatinase B at sites of inflammation may facilitate the establishment of considerable IL-8 activity and localized degradation of the ECM. Whereas neutrophil gelatinase B may be retarded as a consequence of binding of galectin-3 to the ECM, cancer cell gelatinase B may more easily diffuse into the extracellular matrix away from the cells from which it was secreted. This would lead to more widespread matrix degradation, thus facilitating cancer cell invasion and angiogenic growth. By altering its glycosylation, cancer cells may secrete a form of gelatinase B that facilitates cancer progression in a manner that complements that of neutrophil gelatinase B.

MATERIALS AND METHODS

Sample Preparation. Human neutrophil (*11*, *39*) and THP-1 gelatinase B (*31*) were purified as previously described. The human MCF-7 breast cancer cells were incubated for 48 h at 37 °C in serum free Dulbecco's minimal essential medium containing 10 ng/mL phorbol 12-myristate 13-acetate (PMA). Cell supernatants were harvested, filtered, and purified by affinity chromatography on gelatin−Sepharose as previously described (*11*).

In-Gel Enzymatic Release of N-Linked Glycans. Purified gelatinase B samples were reduced and alkylated prior to

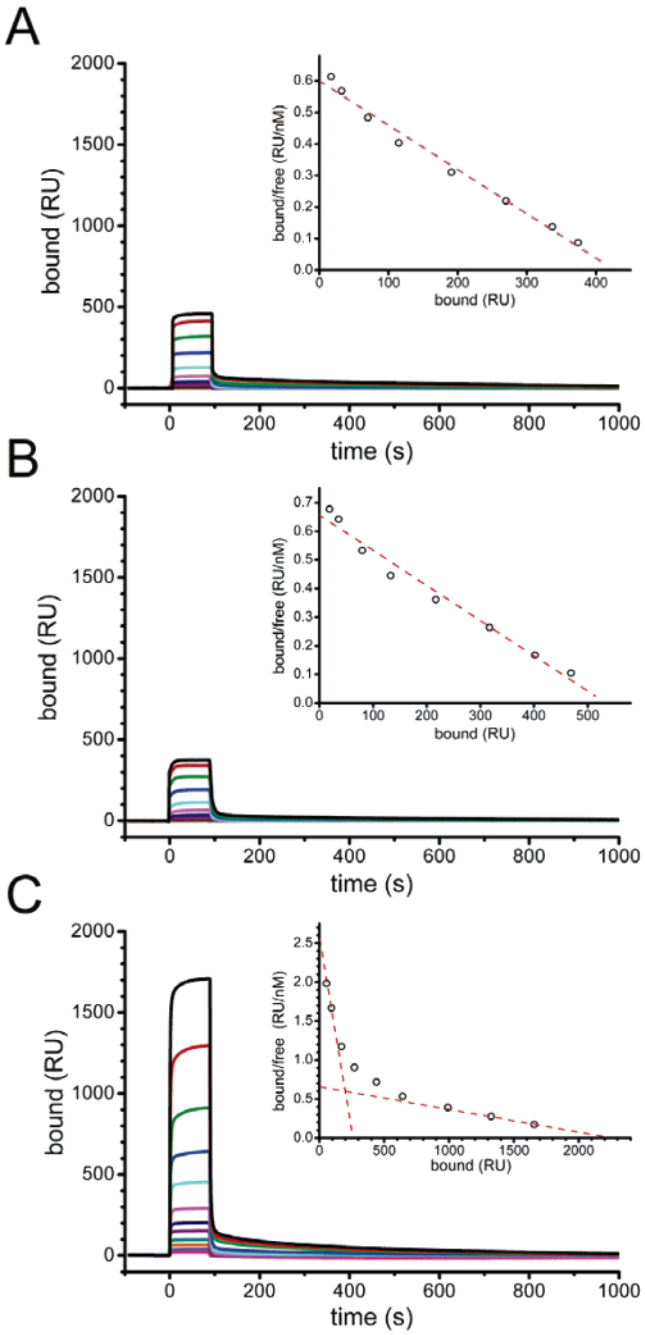

FIGURE 8: Surface plasmon resonance analysis of binding of galectin-3 to gelatinase B. The binding of galectin-3 to immobilized gelatinase B derived from THP-1 cells (A), MCF-7 cells (B), and neutrophils (C) was tested over a range of ligand concentrations: 10 μM (black), 5 μM (red), 2.5 μM (green), 1.25 μM (blue), 625 nM (cyan), 312 nM (magenta), 156 nM (navy), 78 nM (purple), 39 nM (dark cyan), 20 nM (orange), 10 nM (violet), and 5 nM (pink). For each panel, the SPR sensorgram is shown and the Scatchard analysis of that binding is added in the inset to allow for a qualitative (visual) interpretation of the data. K_d and B_{max} values and the errors for those values were calculated from nonlinear curve fits of the Langmuir isotherms. The interaction of galectin-3 with THP-1- or MCF-7-derived gelatinase B shows homogeneous binding character with K_d and B_{max} values of 810 $\pm$ 30 nM and 440 $\pm$ 10 RU, and 920 $\pm$ 20 nM and 560 $\pm$ 12 RU, respectively. The interaction with neutrophil-derived gelatinase B shows a marked biphasicity to the interaction (panel C, inset), best described by two components with K_d and B_{max} values of 110 $\pm$ 30 nM and 170 $\pm$ 30 RU, and 3.3 $\pm$ 0.3 μM and 2070 $\pm$ 40 RU, respectively.

SDS−PAGE. Gel bands were cut out and washed alternatively with 20 mM sodium bicarbonate and acetonitrile. *N*-Glycans were removed from protein in the gel bands by overnight incubation with peptide *N*-glycosidase F (PNGase F) at 37 °C. N-Linked glycans were recovered from the gel pieces with water and sonication before being dried and labeled with 2-aminobenzamide (2-AB).

O-Glycan Release. Manual hydrazinolysis for the selective release of *O*-glycans was performed as previously described (*32*). Briefly, gelatinase B samples were dialyzed against 0.1% trifluoroacetic acid for 24 h at 4 °C, lyophilized, and then cryogenically dried. O-Linked glycans were released by incubation with anhydrous hydrazine for 6 h at 60 °C. *O*-Glycans were then re-*N*-acetylated and desalted, and peptides were removed. Samples were then dried prior to 2-AB labeling.

2-Aminobenzamide Fluorescent Labeling of Released Glycans. Dried glycans were fluorescently labeled with 2-AB according to the method of Bigge et al. (*40*) using a Ludger Tag 2-AB labeling kit (Ludger Limited, Oxford, U.K.). Excess label was removed by ascending chromatography on Whatmann 3MM chromatography paper in acetonitrile. Glycans were washed from the paper with water.

Simultaneous Exoglycosidase Digests. Glycan aliquots (~20 pmol) were evaporated to dryness before the addition of 10 μL of standardized exoglycosidase solutions and incubation for 18 h at 37 °C in the manufacturer's (Prozyme) recommended buffers. Conditions for the individual exoglycosidases in the arrays were as follows: 1−2 units/mL *Arthrobacter ureafaciens* sialidase (ABS, EC 3.2.1.18), 3 milliunits/mL almond meal α-fucosidase (AMF, EC 3.2.1.111), 1 unit/mL bovine kidney α-fucosidase (BKF, EC 3.2.1.51), and 1−2 units/mL bovine testes β-galactosidase (BTG, EC 3.2.1.23). After digestions, samples were passed through a protein-binding filter (Micropure, EZ centrifugal filter devices, Millipore Corp.) to remove exoglycosidases. Glycans were eluted from filters with water.

HPLC Conditions. Normal phase separations were performed on a 2690 Alliance separation module (Waters, Milford, MA) equipped with a Waters 474 fluorescence detector. Normal phase HPLC was performed using a 4.6 mm × 250 mm TSK Amide-80 column (Anachem, Luton, Beds, U.K.) with the low-salt buffer system previously described (*32*, *41*).

Galectin-3−Gelatinase B Binding Assay. Wells of a 96-well ELISA plate (NUNC) were coated with 2.5 μg of recombinant human galectin-3 (R&D Systems, catalog no. 1154-GA/CF) in 100 μL of assay buffer [100 mM Tris-HCl (pH 7.5), 100 mM NaCl, and 10 mM $CaCl_2$] and incubated at 4 °C overnight. Each well was then blocked with 200 μL of blocking solution (PBS, 0.05% Tween 20, and 1 g/L BSA) and incubated for 2 h at 37 °C with agitation; 100 ng of gelatinase B in 100 μL of assay buffer, 0.001% Tween 20, and 30 mM EDTA (to prevent catalytic activity of gelatinase B) was then added to each well and the mixture incubated for 30 min at 37 °C. Each well was then washed with 5 × 200 μL of washing solution (blocking solution with 30 mM EDTA). Finally, 30 μL of zymography loading buffer [0.125 M Tris-HCl (pH 6.8), 4% SDS, 0.25 M sucrose, and 0.1% bromophenol blue] was added to each well to elute bound gelatinase B. As a positive control for binding, wells were coated with 100 ng of gelatin in 100 μL of assay buffer.

Collagenase Treatment of Galectin-3. C. histolyticum collagenase type II (Sigma, catalog no. C-6885) was

incubated at a 3:1 (w/w) galectin-3:collagenase ratio in assay buffer for 21 h at 37 °C. Galectin-3 cleavage was confirmed by SDS−PAGE.

Gelatin Substrate Zymography. The zymograms that were used were 7.5% acrylamide gels copolymerized with 0.1% gelatin. After electrophoresis, zymograms were placed in washing buffer [50 mM Tris-HCl (pH 7.5), 10 mM $CaCl_2$, 0.02% NaN_3, and 2.5% Triton X-100] for 2 × 20 min at room temperature with gentle agitation, before being incubated for 18 h at 37 °C in incubation buffer [50 mM Tris-HCl (pH 7.5), 10 mM $CaCl_2$, 0.02% NaN_3, and 1% Triton X-100]. Zymograms were then stained with Coomassie blue and destained (*11*).

Surface Plasmon Resonance. All experiments were carried out at 25 °C on a Biacore 2000 instrument (BIAcore AB). Three specific binding surfaces were prepared by coupling gelatinase B purified from MCF-7 cells, THP-1 cells, and neutrophils to a CM5 sensor chip through the standard amine coupling procedure. For each sample, a coupling density of ca. 5000 resonance units was used. A mock coupled surface served as a negative control. Two-fold serial dilutions of galectin-3 (R&D Systems) in 10 mM Hepes (pH 7.4), 150 mM NaCl, 5 mM $CaCl_2$, and 0.005% (v/v) surfactant p20 were injected over the sensor chip at a flow rate of 20 μL/min with a 90 s association phase followed by a 20 min dissociation phase. Double referencing data subtraction methods (*42*) were used prior to analysis of rates and equilibrium binding. A series of measurements were recorded at different flow rates (from 10 to 100 μL/min), and no change in dissociation rates was observed, suggesting ligand rebinding was not significant for these interactions.

Molecular Modeling. Molecular modeling was performed on a Silicon Graphics Fuel workstation using InsightII and Discover (Accelrys Inc., San Diego, CA). Figures were produced using Molscript (*43*). The molecular models of gelatinase B and the constructs were based on the crystal structure of gelatinase A (*5*) and the crystal structure of the N-terminal domains of gelatinase B (*44*) obtained from the Protein Data Bank (*45*). The structures of the N-terminal domains of the models were based on the gelatinase B structure. The structure of the hemopexin domain of the models was based on the equivalent domain in the gelatinase A structure. The distance constraint between the first and last residue of the OG domain was determined to give the appropriate separation of the N- and C-terminal domains, based on analytical ultracentrifugation results. Restrained simulated annealing was then used to generate OG domain structures. N-Linked and O-linked glycan structures, chosen on the basis of the sequencing results, were generated using the database of glycosidic linkage conformations (*46*) and in vacuo energy minimization to relieve unfavorable steric interactions. For the N-linked glycans, Asn−GlcNAc linkage conformations were based on the observed range of crystallographic values (*47*) and the torsion angles around the Asn Cα−Cβ and Cβ−Cγ bonds, being adjusted to eliminate unfavorable steric interactions between the glycans and the protein surface. A similar approach was used for the O-linked Ser and Thr linkages. The entire structure was then energy-minimized. The models of galectin were based on the crystal structure of human galectin-3 (*19*) and docked onto gelatinase B by overlaying the glycan residue in the binding site.

REFERENCES

1. Nagase, H., and Woessner, J. F., Jr. (1999) Matrix metalloproteinases, *J. Biol. Chem. 274*, 21491−4.
2. Egeblad, M., and Werb, Z. (2002) New functions for the matrix metalloproteinases in cancer progression, *Nat. Rev. Cancer 2*, 161−74.
3. Van den Steen, P. E., Dubois, B., Nelissen, I., Rudd, P. M., Dwek, R. A., and Opdenakker, G. (2002) Biochemistry and molecular biology of gelatinase B or matrix metalloproteinase-9 (MMP-9), *Crit. Rev. Biochem. Mol. Biol. 37*, 375−536.
4. Opdenakker, G., Van den Steen, P. E., and Van Damme, J. (2001) Gelatinase B: A tuner and amplifier of immune functions, *Trends Immunol. 22*, 571−9.
5. Morgunova, E., Tuuttila, A., Bergmann, U., Isupov, M., Lindqvist, Y., Schneider, G., and Tryggvason, K. (1999) Structure of human pro-matrix metalloproteinase-2: Activation mechanism revealed, *Science 284*, 1667−70.
6. Van den Steen, P. E., Van Aelst, I., Hvidberg, V., Piccard, H., Fiten, P., Jacobsen, C., Moestrup, S. K., Fry, S., Royle, L., Wormald, M. R., Wallis, R., Rudd, P. M., Dwek, R. A., and Opdenakker, G. (2006) The hemopexin and O-glycosylated domains tune gelatinase B/MMP-9 bio-availability via inhibition and binding to cargo receptors, *J. Biol. Chem. 281*, 18626−18637.
7. Mattu, T. S., Royle, L., Langridge, J., Wormald, M. R., Van den Steen, P. E., Van Damme, J., Opdenakker, G., Harvey, D. J., Dwek, R. A., and Rudd, P. M. (2000) O-Glycan analysis of natural human neutrophil gelatinase B using a combination of normal phase-HPLC and online tandem mass spectrometry: Implications for the domain organization of the enzyme, *Biochemistry 39*, 15695−704.
8. Rudd, P. M., Mattu, T. S., Masure, S., Bratt, T., Van den Steen, P. E., Wormald, M. R., Küster, B., Harvey, D. J., Borregaard, N., Van Damme, J., Dwek, R. A., and Opdenakker, G. (1999) Glycosylation of natural human neutrophil gelatinase B and neutrophil gelatinase B-associated lipocalin, *Biochemistry 38*, 13937−50.
9. Kotra, L. P., Zhang, L., Fridman, R., Orlando, R., and Mobashery, S. (2002) N-Glycosylation pattern of the zymogenic form of human matrix metalloproteinase-9, *Bioorg. Chem. 30*, 356−70.
10. Van den Steen, P. E., Opdenakker, G., Wormald, M. R., Dwek, R. A., and Rudd, P. M. (2001) Matrix remodelling enzymes, the protease cascade and glycosylation, *Biochim. Biophys. Acta 1528*, 61−73.
11. Masure, S., Proost, P., Van Damme, J., and Opdenakker, G. (1991) Purification and identification of 91-kDa neutrophil gelatinase. Release by the activating peptide interleukin-8, *Eur. J. Biochem. 198*, 391−8.
12. Zucker, S., Lysik, R. M., Zarrabi, M. H., and Moll, U. (1993) M_r 92,000 type IV collagenase is increased in plasma of patients with colon cancer and breast cancer, *Cancer Res. 53*, 140−6.
13. Hua, J., and Muschel, R. J. (1996) Inhibition of matrix metalloproteinase 9 expression by a ribozyme blocks metastasis in a rat sarcoma model system, *Cancer Res. 56*, 5279−84.
14. Itoh, T., Tanioka, M., Matsuda, H., Nishimoto, H., Yoshioka, T., Suzuki, R., and Uehira, M. (1999) Experimental metastasis is suppressed in MMP-9-deficient mice, *Clin. Exp. Metastasis 17*, 177−81.
15. Ortega, N., Behonick, D. J., Colnot, C., Cooper, D. N., and Werb, Z. (2005) Galectin-3 is a downstream regulator of matrix metalloproteinase-9 function during endochondral bone formation, *Mol. Biol. Cell 16*, 3028−39.
16. Takenaka, Y., Fukumori, T., and Raz, A. (2004) Galectin-3 and metastasis, *Glycoconjugate J. 19*, 543−9.
17. Lagana, A., Goetz, J. G., Cheung, P., Raz, A., Dennis, J. W., and Nabi, I. R. (2006) Galectin binding to Mgat5-modified N-glycans regulates fibronectin matrix remodeling in tumor cells, *Mol. Cell. Biol. 26*, 3181−93.
18. Barondes, S. H., Castronovo, V., Cooper, D. N., Cummings, R. D., Drickamer, K., Feizi, T., Gitt, M. A., Hirabayashi, J., Hughes, C., Kasai, K., et al. (1994) Galectins: A family of animal β-galactoside-binding lectins, *Cell 76*, 597−8.
19. Seetharaman, J., Kanigsberg, A., Slaaby, R., Leffler, H., Barondes, S. H., and Rini, J. M. (1998) X-ray crystal structure of the human galectin-3 carbohydrate recognition domain at 2.1-Å resolution, *J. Biol. Chem. 273*, 13047−52.
20. Ahmad, N., Gabius, H. J., Andre, S., Kaltner, H., Sabesan, S., Roy, R., Liu, B., Macaluso, F., and Brewer, C. F. (2004) Galectin-3 precipitates as a pentamer with synthetic multivalent

carbohydrates and forms heterogeneous cross-linked complexes, *J. Biol. Chem. 279*, 10841−7.
21. Barboni, E. A., Bawumia, S., and Hughes, R. C. (1999) Kinetic measurements of binding of galectin 3 to a laminin substratum, *Glycoconjugate J. 16*, 365−73.
22. Ochieng, J., Platt, D., Tait, L., Hogan, V., Raz, T., Carmi, P., and Raz, A. (1993) Structure-function relationship of a recombinant human galactoside-binding protein, *Biochemistry 32*, 4455−60.
23. Ochieng, J., Green, B., Evans, S., James, O., and Warfield, P. (1998) Modulation of the biological functions of galectin-3 by matrix metalloproteinases, *Biochim. Biophys. Acta 1379*, 97−106.
24. Feizi, T. (1985) Demonstration by monoclonal antibodies that carbohydrate structures of glycoproteins and glycolipids are onco-developmental antigens, *Nature 314*, 53−7.
25. Granovsky, M., Fata, J., Pawling, J., Muller, W. J., Khokha, R., and Dennis, J. W. (2000) Suppression of tumor growth and metastasis in Mgat5-deficient mice, *Nat. Med. 6*, 306−12.
26. Kim, Y. J., and Varki, A. (1997) Perspectives on the significance of altered glycosylation of glycoproteins in cancer, *Glycoconjugate J. 14*, 569−76.
27. Lloyd, K. O., Burchell, J., Kudryashov, V., Yin, B. W., and Taylor-Papadimitriou, J. (1996) Comparison of O-linked carbohydrate chains in MUC-1 mucin from normal breast epithelial cell lines and breast carcinoma cell lines. Demonstration of simpler and fewer glycan chains in tumor cells, *J. Biol. Chem. 271*, 33325−34.
28. Saitoh, O., Wang, W. C., Lotan, R., and Fukuda, M. (1992) Differential glycosylation and cell surface expression of lysosomal membrane glycoproteins in sublines of a human colon cancer exhibiting distinct metastatic potentials, *J. Biol. Chem. 267*, 5700−11.
29. Houde, M., de Bruyne, G., Bracke, M., Ingelman-Sundberg, M., Skoglund, G., Masure, S., van Damme, J., and Opdenakker, G. (1993) Differential regulation of gelatinase B and tissue-type plasminogen activator expression in human Bowes melanoma cells, *Int. J. Cancer 53*, 395−400.
30. Opdenakker, G., Masure, S., Grillet, B., and Van Damme, J. (1991) Cytokine-mediated regulation of human leukocyte gelatinases and role in arthritis, *Lymphokine Cytokine Res. 10*, 317−24.
31. Van Ranst, M., Norga, K., Masure, S., Proost, P., Vandekerckhove, F., Auwerx, J., Van Damme, J., and Opdenakker, G. (1991) The cytokine-protease connection: Identification of a 96-kD THP-1 gelatinase and regulation by interleukin-1 and cytokine inducers, *Cytokine 3*, 231−9.
32. Royle, L., Mattu, T. S., Hart, E., Langridge, J. I., Merry, A. H., Murphy, N., Harvey, D. J., Dwek, R. A., and Rudd, P. M. (2002) An analytical and structural database provides a strategy for sequencing O-glycans from microgram quantities of glycoproteins, *Anal. Biochem. 304*, 70−90.
33. Dalziel, M., Whitehouse, C., McFarlane, I., Brockhausen, I., Gschmeissner, S., Schwientek, T., Clausen, H., Burchell, J. M., and Taylor-Papadimitriou, J. (2001) The relative activities of the C2GnT1 and ST3Gal-I glycosyltransferases determine O-glycan structure and expression of a tumor-associated epitope on MUC1, *J. Biol. Chem. 276*, 11007−15.
34. Shimodaira, K., Nakayama, J., Nakamura, N., Hasebe, O., Katsuyama, T., and Fukuda, M. (1997) Carcinoma-associated expression of core 2 β-1,6-N-acetylglucosaminyltransferase gene in human colorectal cancer: Role of O-glycans in tumor progression, *Cancer Res. 57*, 5201−6.
35. Ihara, S., Miyoshi, E., Ko, J. H., Murata, K., Nakahara, S., Honke, K., Dickson, R. B., Lin, C. Y., and Taniguchi, N. (2002) Prometastatic effect of N-acetylglucosaminyltransferase V is due to modification and stabilization of active matriptase by adding β1-6 GlcNAc branching, *J. Biol. Chem. 277*, 16960−7.
36. Dennis, J. W., Laferte, S., Waghorne, C., Breitman, M. L., and Kerbel, R. S. (1987) β1-6 branching of Asn-linked oligosaccharides is directly associated with metastasis, *Science 236*, 582−5.
37. Fernandes, B., Sagman, U., Auger, M., Demetrio, M., and Dennis, J. W. (1991) β1-6 branched oligosaccharides as a marker of tumor progression in human breast and colon neoplasia, *Cancer Res. 51*, 718−23.
38. Hirabayashi, J., Hashidate, T., Arata, Y., Nishi, N., Nakamura, T., Hirashima, M., Urashima, T., Oka, T., Futai, M., Muller, W. E., Yagi, F., and Kasai, K. (2002) Oligosaccharide specificity of galectins: A search by frontal affinity chromatography, *Biochim. Biophys. Acta 1572*, 232−54.
39. Van den Steen, P. E., Proost, P., Wuyts, A., Van Damme, J., and Opdenakker, G. (2000) Neutrophil gelatinase B potentiates interleukin-8 tenfold by aminoterminal processing, whereas it degrades CTAP-III, PF-4, and GRO-α and leaves RANTES and MCP-2 intact, *Blood 96*, 2673−81.
40. Bigge, J. C., Patel, T. P., Bruce, J. A., Goulding, P. N., Charles, S. M., and Parekh, R. B. (1995) Nonselective and efficient fluorescent labeling of glycans using 2-amino benzamide and anthranilic acid, *Anal. Biochem. 230*, 229−38.
41. Guile, G. R., Rudd, P. M., Wing, D. R., Prime, S. B., and Dwek, R. A. (1996) A rapid high-resolution high-performance liquid chromatographic method for separating glycan mixtures and analyzing oligosaccharide profiles, *Anal. Biochem. 240*, 210−26.
42. Myszka, D. G. (1999) Improving biosensor analysis, *J. Mol. Recognit. 12*, 279−84.
43. Kraulis, P. J. (1991) Molscript: A program to produce both detailed and schematic plots of protien structures, *J. Appl. Crystallogr. 24*, 946−50.
44. Elkins, P. A., Ho, Y. S., Smith, W. W., Janson, C. A., D'Alessio, K. J., McQueney, M. S., Cummings, M. D., and Romanic, A. M. (2002) Structure of the C-terminally truncated human ProMMP9, a gelatin-binding matrix metalloproteinase, *Acta Crystallogr. D58*, 1182−92.
45. Berman, H. M., Westbrook, J., Feng, Z., Gilliland, G., Bhat, T. N., Weissig, H., Shindyalov, I. N., and Bourne, P. E. (2000) The Protein Data Bank, *Nucleic Acids Res. 28*, 235−42.
46. Wormald, M. R., Petrescu, A. J., Pao, Y. L., Glithero, A., Elliott, T., and Dwek, R. A. (2002) Conformational studies of oligosaccharides and glycopeptides: Complementarity of NMR, X-ray crystallography, and molecular modelling, *Chem. Rev. 102*, 371−86.
47. Petrescu, A. J., Milac, A. L., Petrescu, S. M., Dwek, R. A., and Wormald, M. R. (2004) Statistical analysis of the protein environment of N-glycosylation sites: Implications for occupancy, structure, and folding, *Glycobiology 14*, 103−14.

BI061254L